Thermal stability and mechanical properties of hybrid materials based on nitrocellulose grafted by aminopropylisobutyl polyhedral oligomeric silsesquioxane*)

Xiaomei Yang[1)], Yiliang Wang[1)], Yuanyuan Li[1)], Zhipeng Li[1)], Tianyou Song[1)], Xiu Liu[1)], Jianwei Hao[1), **)]

DOI: dx.doi.org/10.14314/polimery.2017.576

Abstract: The need for improvement in nitrocellulose (NC) storage safety and convenience of application requires an increase in NC thermal stability and enhancement of its mechanical properties. To this aim, hybrid materials were synthesized by grafting NC with aminopropylisobutyl polyhedral oligomeric silsesquioxane (amino-POSS) using isophorone diisocyanate (IPDI) as a crosslinking agent. The structure and elemental composition of the resulting products were confirmed by Fourier transform infrared spectroscopy (FT-IR), nuclear magnetic resonance (^{1}H NMR and ^{29}Si NMR), X-ray diffraction (XRD), and X-ray photoelectron spectroscopy (XPS). It was found, based on the silicon mapping using energy dispersive X-ray spectroscopy (EDS), that amino-POSS was well dispersed in NC matrix. Differential scanning calorimetry (DSC) and thermogravimetric analysis (TGA) studies showed that hybrid amino-POSS-NC materials have higher thermal decomposition activation energy (E_a) compared to NC control sample. According to TGA results, the temperatures of 5 % weight loss ($T_{5\,\%}$) and 50 % weight loss ($T_{50\,\%}$) as well as the residual masses at 240 °C ($CR_{240\,°C}$), were increased as a result of NC modification with amino-POSS. As can be seen from the digital and scanning electron microscopy (SEM) images, the char layers of amino-POSS-NC hybrid materials after burning in air became more compact with increasing amino-POSS content. XPS studies have shown an increased content of the graphitized carbon in the char residues of the modified samples. The results of DSC, TGA, SEM and XPS studies have directly proved the enhancement of the thermal stability of amino-POSS-NC hybrid materials. In addition, tensile strengths and Young's moduli of amino-POSS-NC hybrid materials were increased gradually with the amino-POSS content in the uniaxial tensile tests. All these results show that the proposed modification of nitrocellulose improves the safety of manufacture and use of this material.

Keywords: nitrocellulose, hybrid material, aminopropylisobutyl polyhedral oligomeric silsesquioxane, thermal stability, mechanical properties.

Stabilność termiczna i właściwości mechaniczne materiałów hybrydowych na bazie nitrocelulozy szczepionej oligomerycznym wielofunkcyjnym aminopropyloizobutylosilseskwioksanem

Streszczenie: Poprawa bezpieczeństwa przechowywania nitrocelulozy (NC) wymaga zwiększenia jej stabilności termicznej, a wygoda używania poprawy właściwości mechanicznych. W tym celu zsyntetyzowano materiały hybrydowe, w których NC szczepiono oligomerycznym wielofunkcyjnym aminopropyloizobutylosilseskwioksanem (amino-POSS) stosując jako środek sieciujący izoforonodiizocyjanian (IPDI). Strukturę i skład otrzymanych materiałów potwierdzono za pomocą spektroskopii w podczerwieni z transformatą Fouriera (FT-IR), jądrowego rezonansu magnetycznego (^{1}H NMR i ^{29}Si NMR), dyfraktometrii rentgenowskiej (XRD) oraz spektroskopii fotoelektronów rentgenowskich (XPS). Na podstawie wyników badań mapowania Si, otrzymanych metodą spektroskopii dyspersji energii promieniowania rentgenowskiego (EDS), stwierdzono, że amino-POSS został dobrze zdysper-

[1)] Beijing Institute of Technology, School of Materials Science and Engineering, National Engineering Technology Research Center of Flame Retardant Materials, Beijing 100081, PR China.

*) This material was presented at 9th International Conference MoDeSt 2016, 4–8 September 2016, Cracow, Poland.

**) Author for correspondence; e-mail: hjw@bit.edu.cn

gowany w matrycy NC. Badania stabilności termicznej przeprowadzone za pomocą różnicowej kalorymetrii skaningowej (DSC) wykazały, że materiały hybrydowe typu amino-POSS-NC charakteryzują się większymi wartościami energii aktywacji rozkładu termicznego (E_a) niż próbka kontrolna NC. Zgodnie z wynikami analizy termograwimetrycznej (TGA) wartości temperatury ubytku 5 % ($T_{5\ \%}$) i 50 % ($T_{50\ \%}$) masy próbki oraz pozostałości masy w temperaturze 240 °C ($CR_{240\ °C}$) zwiększały się na skutek modyfikacji NC za pomocą amino-POSS. Według fotografii cyfrowych i fotografii wykonanych metodą skaningowej mikroskopii elektronowej (SEM) warstwy węglowe powstałe po spaleniu materiałów hybrydowych w powietrzu wraz ze zwiększeniem zawartości amino-POSS stawały się coraz bardziej zwarte, a wyniki badań XPS wykazały, że tworzyło się coraz więcej węgla w postaci grafitu. Wszystkie wyniki DSC, TGA, SEM i XPS dowodzą poprawy stabilności termicznej materiałów hybrydowych amino-POSS-NC. Stwierdzono także, że wytrzymałość na rozciąganie i moduł Young'a podczas prób jednoosiowego rozciągania materiałów hybrydowych rosną ze zwiększaniem się zawartości amino-POSS. Wyniki wszystkich przeprowadzonych badań dowodzą, że zaproponowana modyfikacja NC poprawia bezpieczeństwo wytwarzania i użytkowania tych materiałów w porównaniu z niemodyfikowanym NC.

Słowa kluczowe: nitroceluloza, materiał hybrydowy, oligomeryczny wielofunkcyjny aminopropyloizobutylosilseskwioksan, stabilność termiczna, właściwości mechaniczne.

Nitrocellulose (NC) is the nitrate ester of cellulose [1], which comes from the nitration of the natural material. It can be used in various applications based on the different nitrogen contents [2, 3]. The main applications of NC with low nitrogen content [4] are in the fields of coatings [5], printings [6], membranes [7], magnetic filtrations [8], and others [9, 10]. Although NC products present many outstanding features (*e.g.*, transparence and fast drying [11]), the poor thermal stability limits their application because NC has spontaneous ignition property and it is susceptible to combust [12, 13] (high burning rate, no residual char [14]). Additionally, the poor mechanical properties of NC [15] also restrict the down-stream products. In terms of the storage safety and the usage requirements, it is essential to endow NC with good thermal stability and mechanical properties, which can be realized by introducing some additives or reactive modifiers into NC.

During the past decades, various additive modifiers, such as diphenylamine (DPA) [16], malonanilide dimers [17] and 1,4-diaminoanthraquinone (DAAQ) [18], have been used to improve the thermal stability of NC. In addition, inorganic salts [19] are also used to increase the thermal stability and prolong the induction time period of NC. However, the migration and poor compatibility are the main problems associated with the additive modifiers prepared in this manner. Compared with the additive modifiers, reactive modifiers are usually incorporated into the backbone of the polymer matrix, increasing the thermal stability in an efficient way [20].

Great scientific interest in polyhedral oligomeric silsesquioxane (POSS) has been stimulated by the smallest known silica particles with the specific cage-like molecular structure with inorganic silicon-oxygen core (Si_8O_{12}) and eight variable organic vertex groups [21, 22]. The organic substituents endow the POSS with good dispersion and miscibility, which is the key to tailor a wide variety of nano- and micro-structured organic/inorganic hybrid materials [23]. In general, the formation of a ceramic layer on the surface of the materials by POSS thermal degradation resulted in a protective physical barrier, strongly improving the thermal stability [24]. The incorporation of POSS into polymers would enhance obviously their mechanical properties [25], yet retaining the processibility and commodity [26]. Furthermore, POSS derivates also possess various chemical side groups [27], *e.g.*, aminopropylisobutyl polyhedral oligomeric silsesquioxane (amino-POSS), which can facilitate its chemical incorporation into a given polymer *via* chemical method [28].

To the best of our knowledge, using chemical method to graft POSS onto NC has not been reported yet. Thus, in the present study, in aim to improve the thermal stability and mechanical properties of NC, amino-POSS will be grafted onto NC by using isophorone diisocyanate (IPDI) as a linkage, giving rise to a series of amino-POSS-NC hybrid materials containing different amino-POSS contents. IPDI is an aliphatic ring with one primary and one secondary isocyanate group, which has unequal reactivity at different temperatures [29]. We will mainly study the influence of amino-POSS content on the thermal stability and mechanical properties of NC materials.

EXPERIMENTAL PART

Materials

Nitrocellulose (NC, nitrogen content ~ 11.91 wt %) was kindly provided by Baoding BaoFeng Nitrocellulose Co., Ltd (Hebei, China). All NC was pre-treated to remove residual water in a freeze dryer at -80 °C for 48 h and stored in a desiccator before use.

Isophorone diisocyanate (IPDI) and tin(II) 2-ethylhexanoate [$Sn(Oct)_2$] were purchased from Alfa Aesar.

Aminopropylisobutyl polyhedral oligomeric silsesquioxane (amino-POSS, 99.98 %) was purchased from Hybrid Plastics.

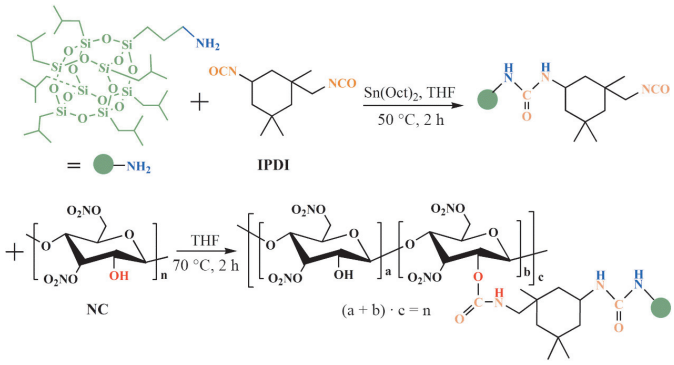

Scheme A. The synthetic route of amino-POSS-NC hybrid materials

Tetrahydrofuran (THF) and *n*-hexane were purified by distillation over CaH_2.

All other reagents were obtained from Beijing Chemical Works and used as received.

Preparation of amino-POSS-NC hybrid materials

$Sn(Oct)_2$ (volume conc. = 0.0013 g/cm^3) was added to a three-necked flask containing amino-POSS in THF (30 cm^3). Then, stoichiometric amount of IPDI with 10 cm^3 THF was dropped into the flask. The stirring was continued at 50 °C for 2 h. Subsequently, appropriate amount of NC solution (in 30 cm^3 THF) was added to the mixture and then the mixture was heated up to 70 °C. The reaction was kept for additional 2 h. All above operations were carried out under a nitrogen atmosphere. At last, the amino-POSS-NC hybrid materials were precipitated in a 5-fold amount of *n*-hexane for three times. After drying, light yellow solids were obtained. The synthetic route of preparation of NC grafted with amino-POSS are presented in Scheme A, and the detailed recipes are listed in Table 1. The yields of syntheses performed using 8.9 wt %, 22.1 wt % and 31.2 wt % amino-POSS-NC are 86.9 %, 84.7 % and 87.6 %, respectively.

The NC control and amino-POSS-NC hybrid material films were obtained through mixing NC or amino-POSS-NC hybrid materials with butanone solution (0.1 g/cm^3). The mixtures were casted to polytetrafluoroethylene substrates, allowed to evaporate at ambient temperature for 48 h, and then dried at 50 °C in a vacuum oven for another 24 h. The average thickness of the resulting films was 1 mm, which can be controlled by the amount of solution used.

Methods of testing

Fourier transform infrared spectroscopy (FT-IR) was applied in the range of 4000–400 cm^{-1} with Bruker Tensor-27 FT-IR spectrometer at room temperature using the KBr disk method.

Nuclear magnetic resonance (^{1}H NMR and ^{29}Si NMR) spectra were recorded at room temperature on AV400 (Bruker) NMR instrument with DMSO-d_6 as solvent and tetramethylsilane (TMS) as internal standard.

T a b l e 1. Preparation of NC control sample and amino-POSS-NC hybrid materials

Sample symbol	NC, wt %	IPDI, wt %	Amino-POSS, wt %
NC (control sample)	100	0	0
H1	89.3	1.8	8.9
H2	73.5	4.4	22.1
H3	62.5	6.3	31.2

X-ray diffraction analysis (XRD) was performed using an *X'*pert PRO diffractometer system. CuK_α radiation was used with a copper target over the 2θ range of 5–40° at a speed of 10 °/min.

X-ray photoelectron spectroscopy (XPS) was applied using a PHI Quantera II SXM at 25 W, under a vacuum of $2.6 \cdot 10^{-7}$ Pa with AlK_α X-ray source. Furthermore, the weight content of Si (Si %) for each amino-POSS-NC hybrid material was calculated according to equation:

$$\text{Si}\,\% = \frac{C_A(\text{Si}) \cdot M(\text{Si})}{C_A(\text{C})M(\text{C}) + C_A(\text{O})M(\text{O}) + C_A(\text{N})M(\text{N}) + C_A(\text{Si})M(\text{Si})} \cdot 100\,\% \quad (1)$$

where: C_A(C), C_A(O), C_A(N), C_A(Si) – the atomic concentrations of C, N, O and Si elements on the surface and the char residues of amino-POSS-NC hybrid material, respectively; *M*(C), *M*(O), *M*(N), *M*(Si) – the relative atomic mass of C, O, N and Si elements.

The spectrometer was calibrated using the binding energy of adventitious carbon as 284.6 eV.

Differential scanning calorimetry (DSC) was carried out on Netzsch 200 PC instrument. All the samples were heated from room temperature to 200 °C at the heating rate of 2, 5, 7 or 10 °C/min with a continuous N_2 flow rate of 60 cm^3/min. The sample mass in the pan was around 5.0 mg.

Thermogravimetric analysis (TGA) was performed using Netzsch TG 209 with a continuous flow of a N_2 atmosphere. Samples (~ 3.0 mg) were heated from 50 °C to 240 °C at a rate of 10 °C/min. The following parameters were determined: initial decomposition temperature based on 5 % mass loss ($T_{5\,\%}$), middle decomposition temperature based on 50 % mass loss ($T_{50\,\%}$) and char residues under 240 °C ($CR_{240\,°C}$).

Scanning electron microscopy (SEM) was applied by using Hitachi S-4700 SEM apparatus. In addition, the distribution of Si atoms was obtained by energy dispersive X-ray spectroscopy (EDS) Si mapping.

Uniaxial tensile tests were carried out on Instron 1185 at 25 °C with a crosshead speed of 5 mm/min. Rectangular tensile bars measuring 50 mm x 10 mm x 1 mm were obtained above using a fresh razor blade.

RESULTS AND DISCUSSION

Chemical structure characterization

The FT-IR spectra of NC (control sample) and amino-POSS-NC hybrid materials are presented in Fig. 1a. Two characteristic peaks at 1661 cm^{-1} and 1284 cm^{-1} are attributed to NO_2 asymmetric and symmetric stretching vibrations, respectively, while the group at 840 cm^{-1} is related to the O-NO_2 vibrations [30]. The increase in the peak intensity at 1661 cm^{-1} for amino-POSS-NC hybrid materials is also attributed to the C=O stretching vibration (amide I). The successful grafting of amino-POSS onto NC can be confirmed by the appearance of dominant Si-O-Si stretching vibration at 1109 cm^{-1} and 482 cm^{-1} [31, 32]. The intensity of the bands of saturated C-H bonds is increased when compared with NC control, further indicating the introduction of amino-POSS. In addition, the peak Q in Fig. 1a shifts from 3558 cm^{-1} (NC) to 3406 cm^{-1} (H3). It is because the peak corresponding to asymmetric stretching vibration of N-H in amide, near 3400 cm^{-1} [33] is formed, and the introducing of amino-POSS with significant steric hindrance may impair the interaction of intermolecular hydrogen bond of NC.

The ^{1}H NMR spectra of NC and H3 amino-POSS-NC hybrid material are shown in Fig. 1b. The resonance peaks at 0.58 ppm (peak 1), 0.93 ppm (peak 2), and 1.80 ppm (peak 3) are caused by seven isobutyl hydrocarbon substituents of the amino-POSS [34]. The multiple resonances at peak 2 (δ 0.8–1.0 ppm) and peak 1 (δ 0.58 ppm) in H3 amino-POSS-NC hybrid material correspond to the chemical shifts of methyl (CH_3) and methylene (CH_2) of amino-POSS, respectively. Moreover, the enhanced peak 3 (δ 1.80 ppm) is methine (CH) group of amino-POSS [31]. These results give a further proof of the grafting reaction.

The ^{29}Si NMR spectrum of H3 amino-POSS-NC hybrid material is shown in Fig. 1c. The signal of Si (-67.88 ppm) was detected indicating the successful synthesis of amino-POSS-NC.

The XRD patterns of NC, H3 amino-POSS-NC hybrid material and amino-POSS are presented in Fig. 2. Both NC and H3 samples show a wide, amorphous diffraction peak at 2θ ≈ 20°, which is attributed to the characteristic peak of NC [35]. As compared with NC control sample, H3 amino-POSS-NC shows a diffraction peak at 2θ ≈ 9° after washing with *n*-hexane for removing the unreacted substances, indicating that the amino-POSS is grafted onto NC. Notably, this peak is related to the local order among amino-POSS molecules of the Si-O-Si caged structure [36].

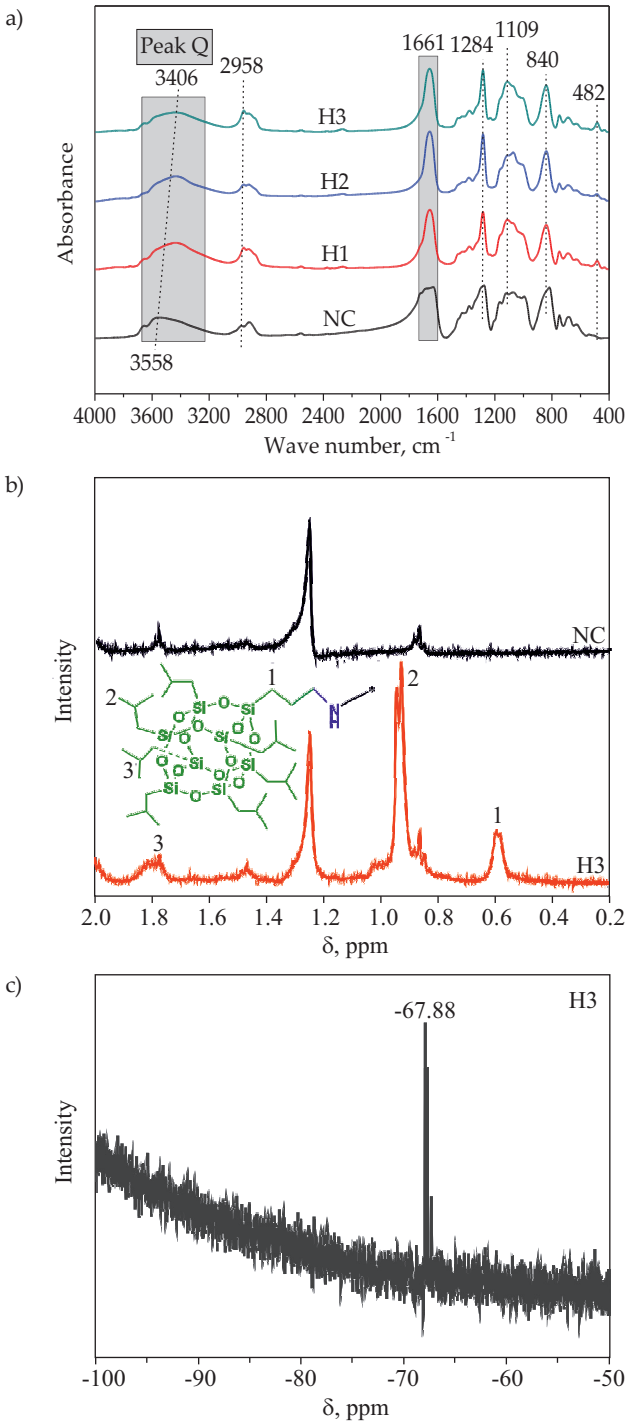

Fig. 1. Spectra of NC (control sample) and amino-POSS-NC hybrid materials: a) FT-IR, b) ^{1}H NMR, c) ^{29}Si NMR

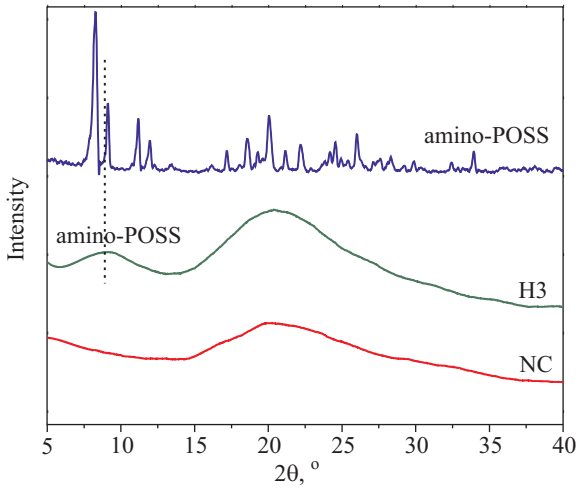

Fig. 2. XRD spectra of NC, H3 amino-POSS-NC hybrid material and amino-POSS

T a b l e 2. Elemental compositions of the surface for NC control sample and amino-POSS-NC hybrid materials

Sample symbol	Atomic concentration, %				Content of Si, wt %
	C	N	O	Si	
NC	70.1	1.7	28.2	0	0
H1	63.9	5.6	25.7	4.8	9.7
H2	67.3	2.8	19.1	10.8	20.8
H3	66.2	2.3	20.3	11.2	21.3

The changes in elemental composition of the surfaces for NC control and amino-POSS-NC hybrid materials were determined using XPS and the corresponding data are listed in Table 2. As it can be seen, the increasing content of Si calculated from atomic concentration of C, N, O, Si demonstrates the increase of amino-POSS content in the NC matrix.

Fracture morphology and dispersion of amino-POSS

The fracture surface SEM images of NC and amino--POSS-NC hybrid materials are shown in Fig. 3. The fracture of NC is smooth because of brittle failure. When amino-POSS is added to the NC matrix, rough fracture morphologies can be observed. This is probably because the amino-POSS can restrain the crack propagation to some extent and change the torturous path of the propagating crack, contributing accordingly to the higher fracture roughness than that of NC [37, 38]. The EDS Si mappings of amino-POSS-NC hybrid materials at each top right corner of Fig. 3b–3d show that the amino-POSS is well dispersed throughout the NC matrix. This enhanced dispersion can be attributed to the introduction of the amino-POSS at molecular-level by IPDI linkage.

Thermal stability

DSC measurements were performed to evaluate the thermal stability of NC and amino-POSS-NC hybrid materials. Figure 4a shows the DSC curves of NC control sample (being taken as a typical example) at 2, 5, 7 and 10 °C/min heating rates. It is found that with the increasing heating rate, the decomposition of the NC shifts to a higher temperature which is consistent with the result in the literature [39]. The corresponding data at peak temperature of the four investigated samples are listed in Table 3. To compare the thermal reactivities of NC and amino-POSS-NC hybrid materials, we set up a simple relationship using Ozawa model [40, 41] between the exothermic peak temperature (T_{peak}), constant heating rate (β), thermal decomposition activation energy (E_a), and universal gas constant (R):

$$\log\beta + 0.496\frac{E_a}{RT_{peak}} = C \qquad (2)$$

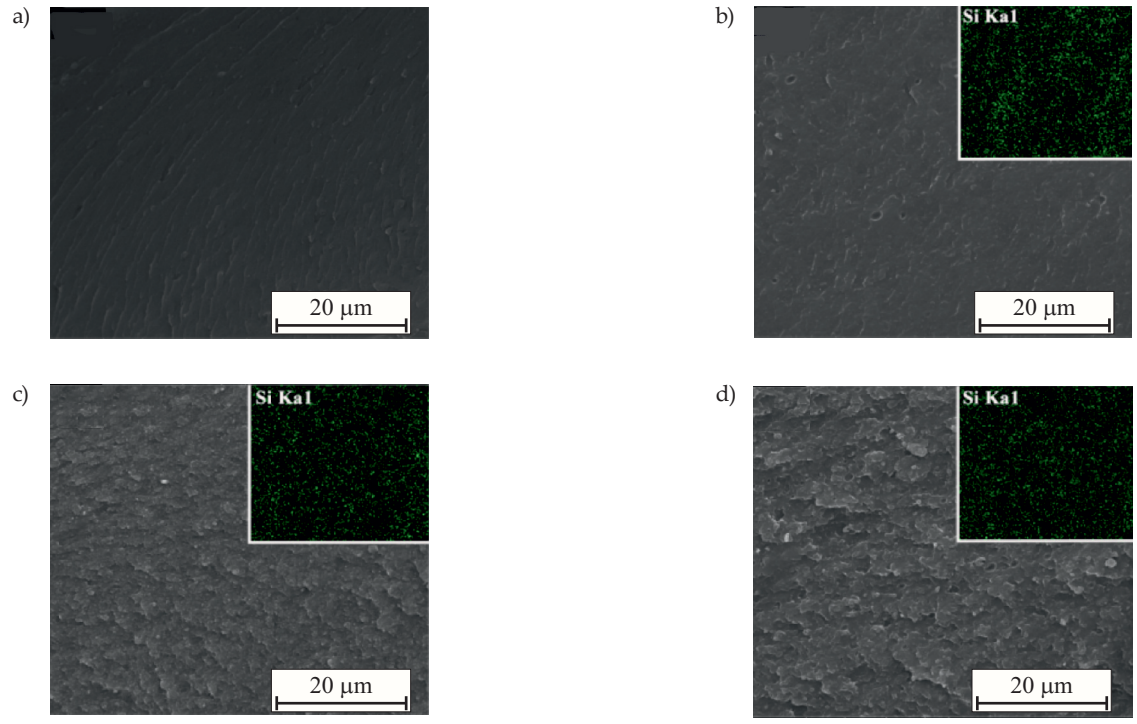

Fig. 3. SEM images of fracture surface and Si mappings by EDS method of: a) NC, b) H1, c) H2, d) H3

As it is shown in Fig. 4b, the plots of the logarithm of β are linear with the reciprocal of the T_{peak}. By applying the Ozawa model, the E_a can be calculated from the slope of the lines.

To further verify the precision of the E_a, Kissinger model [42, 43] was used as a comparable method.

$$\frac{d[\ln(\beta / T_{peak}^2)]}{d(1 / T_{peak})} = -\frac{E_a}{R} \quad (3)$$

As presented in Fig. 4c, the plots of $\ln(\beta / T_{peak}^2)$ against the reciprocal of the T_{peak} are straight lines for NC modified by amino-POSS. Therefore, it can be said that the first-order kinetics offer a good matching of the observed decomposition behavior in this temperature range [44]. The slope of the lines is equal to $-E_a/R$. Thus, the E_a is also obtained from the slope of the graph.

The E_a results, which are calculated from both models, are summarized in Table 3. Comparing the data obtained from the two methods, we found that the values calculated by Kissinger model are slightly higher than those calculated by Ozawa model (Fig. 4d). Furthermore, the E_a of the samples is increased with the increasing of the amino-POSS content, which directly proves the improvement of thermal stability of the modified NC. There are three main reasons for this result:

– the thermally stable compounds with Si-O-Si structure are grafted on the side chain of NC;

– the rigid silica cages can restrain the molecular tumbling and block the degradation of the surrounding molecules [45];

– the introduction of cubic cage structured amino-POSS expands the space between NC chains, which gives rise to lower thermal conductivity [46].

The thermal stability of NC and amino-POSS-NC hybrid materials are further evaluated by TGA under a nitrogen atmosphere. The TGA curves are shown in Fig. 5, and the corresponding data are summarized in Table 4. The $T_{5\ \%}$ values of amino-POSS-NC hybrid materials shift to the temperature higher approximately by 3.0 °C. The $T_{50\ \%}$ values of H1, H2 and H3 amino-POSS-NC hybrid materials shift to the temperatures higher by 3.2 °C, 8.7 °C and 10.6 °C, respectively, which is almost consistent with DSC results above, further indicating that the thermal stability of the amino-POSS-NC hybrid materials is improved. Additionally, the char residues at 240 °C were increased from 1.4 % for NC control sample to 3.1 %,

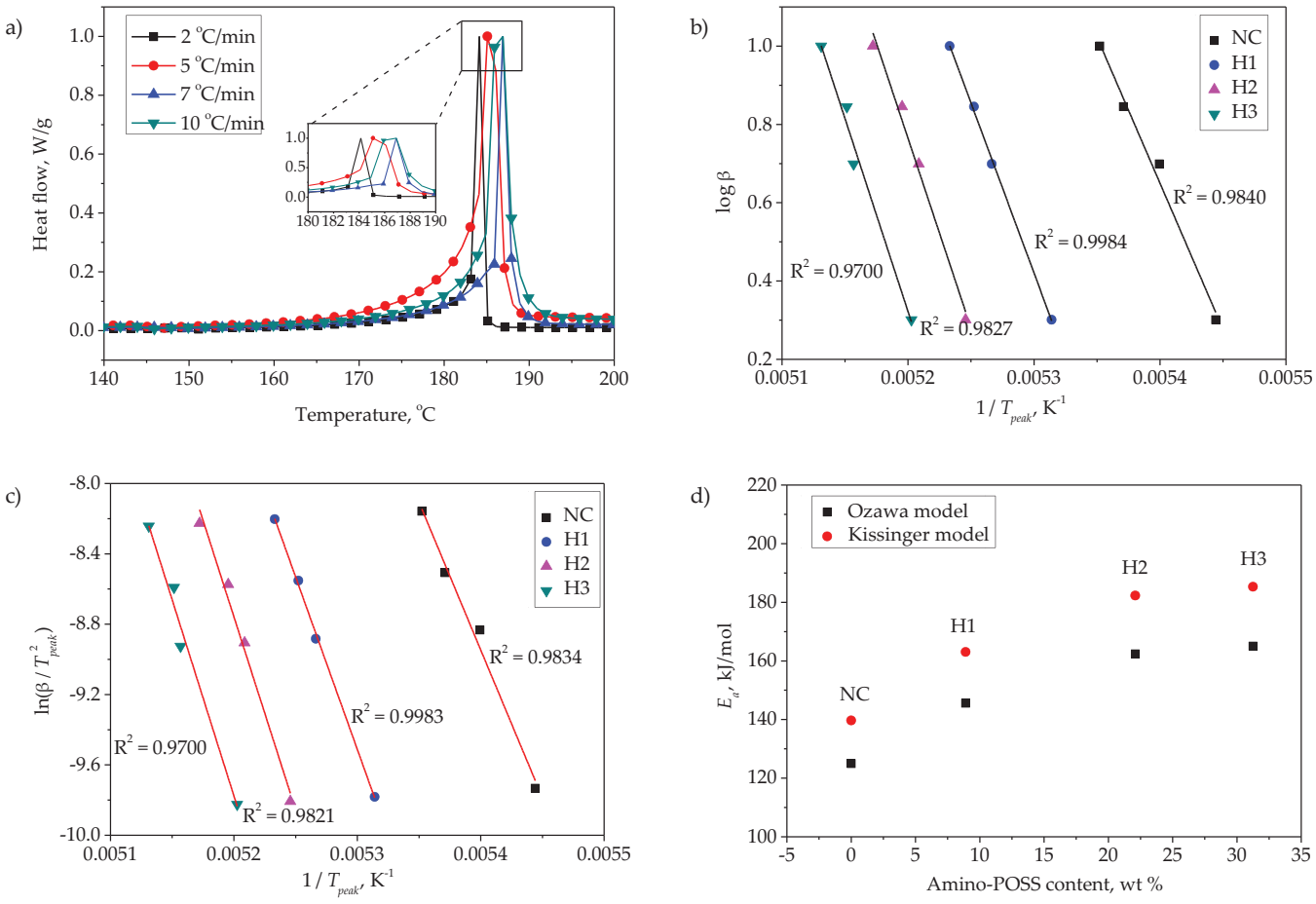

Fig. 4. Effect of different heating rate on the DSC results for NC control sample (a), plots of logβ *versus* the reciprocal of the peak temperature (T_{peak}) for NC and hybrid materials by Ozawa model (b), plots of $\ln(\beta / T^2_{peak})$ *versus* T_{peak} for NC and hybrid materials by Kissinger model (c) and comparison plot of E_a from the both models for NC and hybrid materials (d)

T a b l e 3. DSC data for NC control sample and amino-POSS-NC hybrid materials

Heating rate, °C/min	T_{peak}, °C			
	NC	H1	H2	H3
2	183.7	188.2	190.6	192.2
5	185.2	189.9	192.0	193.9
7	186.2	190.4	192.5	194.1
10	186.8	191.1	193.3	194.9
Model	E_a, kJ/mol			
Ozawa	124.98	145.53	162.41	165.06
Kissinger	139.65	163.06	182.29	185.29

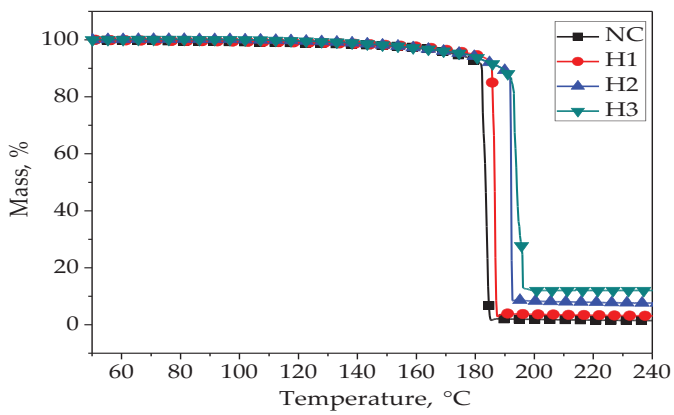

Fig. 5. TGA results for NC control sample and hybrid materials (H1, H2 and H3)

T a b l e 4. TGA results for NC control sample and amino-POSS--NC hybrid materials

Sample symbol	$T_{5\,\%}$, °C	$T_{50\,\%}$, °C	$CR_{240\,°C}$, %
NC	172.9	183.4	1.4
H1	178.7	186.6	3.1
H2	176.2	192.1	7.6
H3	176.3	194.0	12.0

$T_{5\,\%}$ – initial decomposition temperature based on 5 % mass loss, $T_{50\,\%}$ – middle decomposition temperature based on 50 % mass loss, $CR_{240\,°C}$ – char residue at 240 °C.

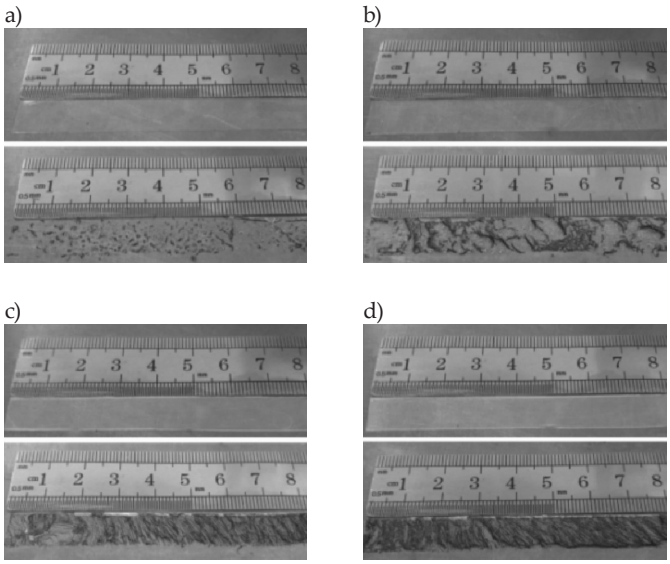

Fig. 6. Digital photographs before (top) and after combustion in air (bottom) of: a) NC, b) H1, c) H2, d) H3

7.6 % and 12.0 % for H1, H2 and H3, respectively. The increase in the char residues gives rise to the formation of more stable char layers, which may protect the materials from further decomposition and in turn increase the thermal stability [47].

The digital photographs of NC sample and amino-POSS--NC hybrid materials before and after combustion in air are shown in Fig. 6. For the NC sample, we can clearly see that

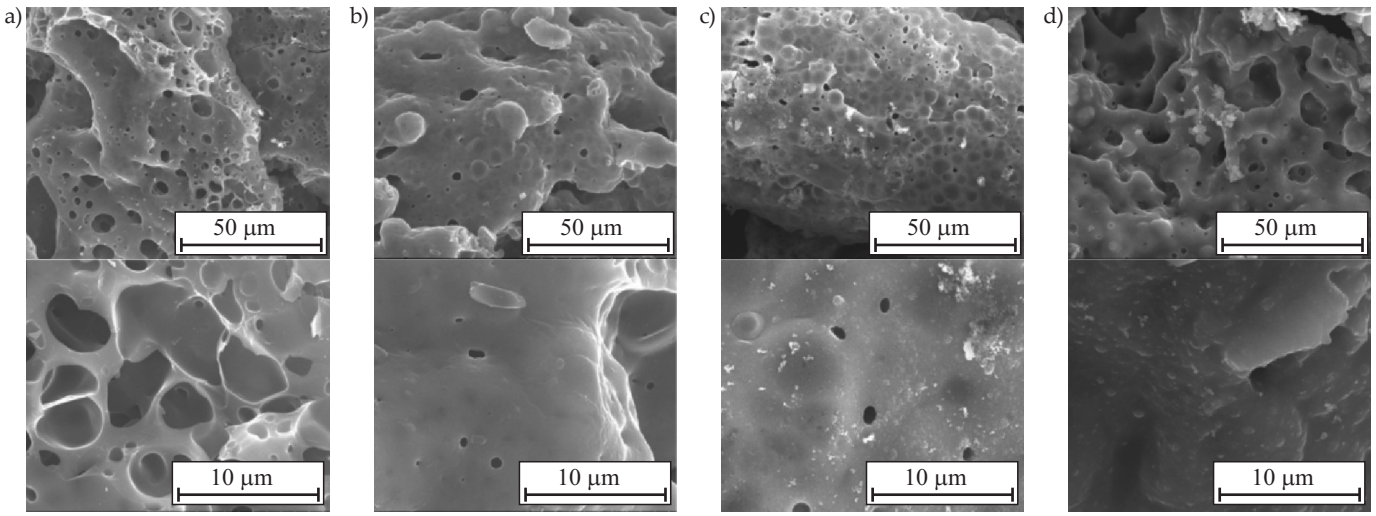

Fig. 7. SEM images for char residues of: a) NC, b) H1, c) H2, d) H3

there are almost no char residues. After grafting amino-POSS onto NC, more char residues are left and the char residues of amino-POSS-NC hybrid materials are increased with the increasing of amino-POSS contents, which is consistent with the TGA result. Furthermore, the morphologies of char residues of the four samples are investigated by SEM and are presented in Fig. 7. The SEM micrographs of char residues of NC control sample, H1, H2 and H3 were made. It can be found that the char residues of NC control sample present the traditional char structure with lots of loose holes, suggesting a poor char quality. As reported, the poor char layer can not effectively act as a barrier protecting the polymer from heating in air [48]. While, with the increasing of amino-POSS content, the detailed surfaces of amino-POSS-NC hybrid materials show a compact and continuous char layer with relative small pores. The increased char residues with compact and continuous char layers, which serve as thermal insulating barriers, inhibit effectively the transmission of heat and mass between NC and the surroundings [49]. This phenomenon further ensures the improvement of thermal stability of NC after modification.

XPS was chosen to analyze the composition changes of the char residues as depicted in Fig. 6. The results are shown in Fig. 8. C1s spectra in Fig. 8 are deconvoluted into four components with fixed positions adopted in the analysis of the C1s region of carbon materials, and the different binding energy (*BE*) of carbon is provided. The components in Table 5 represent graphitic carbon (peak 0, *BE* = 284.4 eV), carbon in hydroxyl, ether groups (peak 1, *BE* = 286.1 eV), carbon in carbonyl groups (peak 2, *BE* = 287.7 eV), and ester groups (peak 3, *BE* = 288.7 eV) [50–52]. After the incorporation of amino-POSS, the content of graphite carbon (area of peak 0) increases from 36.0 % for NC control sample to 59.0, 62.8 and 71.9 % H1, H2 and H3, respectively. It means that more graphite carbons are formed with the increase in amino-POSS content. We suppose that the interaction between amino-POSS, IPDI and NC matrix promotes the formation of more graphitic carbons. In addition, the ratio of oxidized carbons number (*Co*) to non-oxidized carbons number (*Cn*) can be used to indicate the thermal stability of char layer [53], and the ratio values of *Co* to *Cn* (*Co*/*Cn*) of the char residues for the four samples are given in Table 6. It can be seen that the *Co*/*Cn* for H1, H2 and H3 hybrid materials are 0.5, 0.6 and 0.4, respectively, far less than that of NC control (1.1), indicating that the introducing of amino-POSS enhances the thermal stability of char residues for

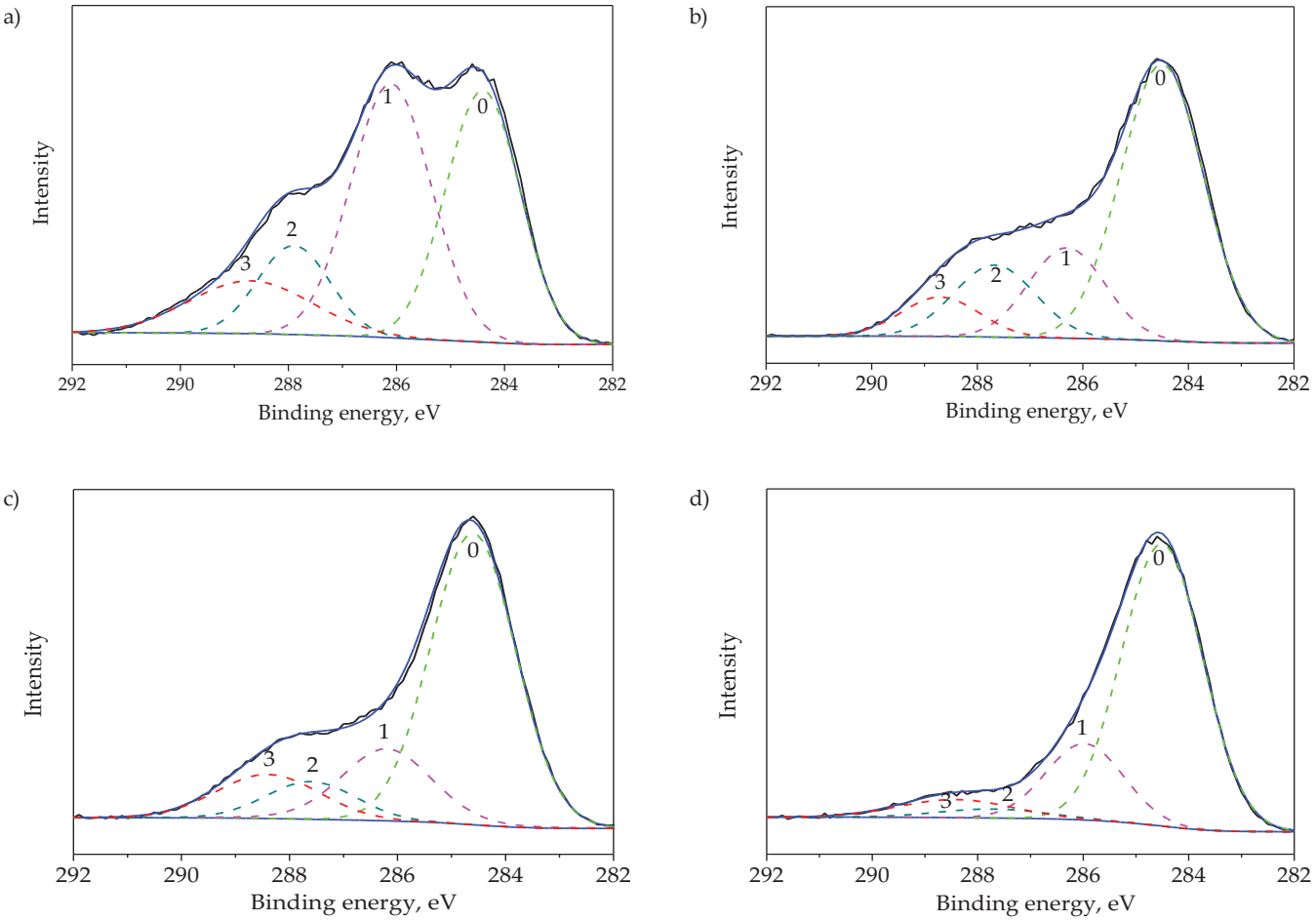

Fig. 8. C1s spectra for char residues after combustion in air: a) NC, b) H1, c) H2, d) H3

T a b l e 5. Cls curve-fitting of char residues for NC control sample and amino-POSS-NC hybrid materials

Peak	NC		H1		H2		H3		Assignment
	BE, eV	*A**), %	*BE*, eV	*A*, %	*BE*, eV	*A*, %	*BE*, eV	*A*, %	
0	284.4	36.0	284.5	59.0	284.6	62.8	284.5	71.9	Graphitic carbon
1	286.1	39.3	286.3	17.9	286.2	17.3	286.3	18.6	R–OH + C–O–C
2	287.9	12.3	287.7	15.2	287.6	8.5	287.7	3.1	>C=O
3	288.7	12.4	288.7	7.9	288.4	11.4	288.7	6.4	–C(=O)–O–

*) A – peak area percentage.

amino-POSS-NC hybrid materials. Moreover, the weight content of Si element (Table 7) in the char residues is accumulated gradually with the increasing content of amino-POSS, further indicating that the amino-POSS has been introduced into the NC, and contributes to the formation of the char residues.

T a b l e 6. The values of *Co*/*Cn* of char residues for NC control sample and amino-POSS-NC hybrid materials

Sample symbol	*Co*/*Cn*
NC	1.1
H1	0.5
H2	0.6
H3	0.4

Mechanical properties

The digital photographs of the NC and amino-POSS-NC hybrid materials are shown in Fig. 9. From the picture we can see that the amino-POSS-NC hybrid materials maintain good elasticity and transparency comparing with that of NC control sample.

Mechanical properties of the four samples are recorded to study the influence of amino-POSS contents on the rigidity and toughness of the material. The stress-strain curves, tensile strengths and Young's moduli of all samples are presented in Fig. 10. The corresponding data are shown in Table 8. As it can be seen, the tensile strengths are increased from 42.9 MPa for NC control sample to 56.8, 64.0 and 74.4 MPa for H1, H2 and H3, respectively. The Young's moduli are increased from 1823 MPa for NC to 2043, 2319 and 2836 MPa for H1, H2 and H3, respectively. The increase in tensile strengths and Young's moduli can be attributed to the good dispersion due to the formation of covalent bond among amino-POSS, IPDI and NC matrix [54]. Additionally, the interaction between amino-POSS [55] may be strengthened with the increasing content of amino-POSS, which can also contribute to the enhancement of tensile strengths and Young's moduli. Notably, an excess of amino-POSS with rigid particles make the material more brittle, resulting in a slight decrease in the elongation at break (*e.g.* for H3), which is consistent with the result reported elsewhere [56].

CONCLUSIONS

In summary, we successfully synthesized the NC hybrid materials by grafting amino-POSS onto NC for improving the thermal stability and mechanical proper-

T a b l e 7. Elemental compositions of char residues for NC control sample and amino-POSS-NC hybrid materials

Sample symbol	Atomic concentration, %				Content of Si, wt %
	C	N	O	Si	
NC	66.5	4.4	29.1	0	0
H1	60.2	3.5	30.7	5.6	10.9
H2	56.8	3.5	31.6	8.1	15.6
H3	45.4	2.9	37.8	13.9	24.6

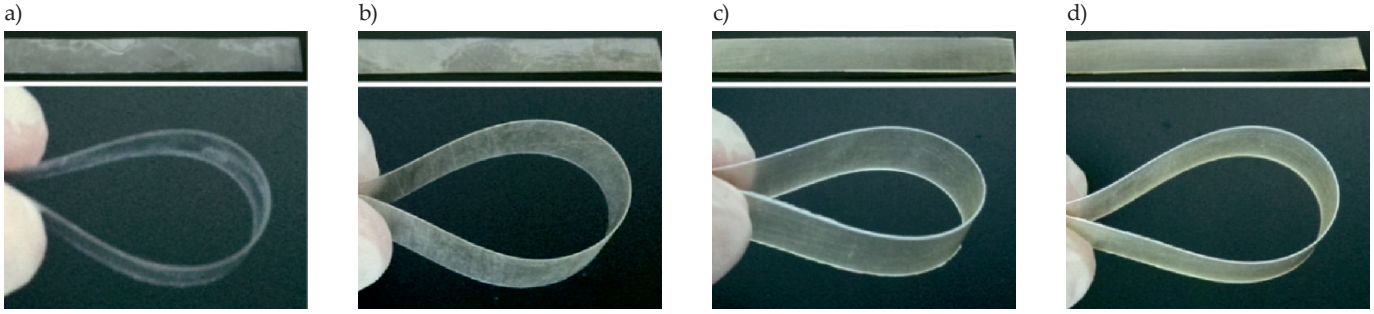

Fig. 9. Digital photographs of: a) NC, b) H1, c) H2, d) H3

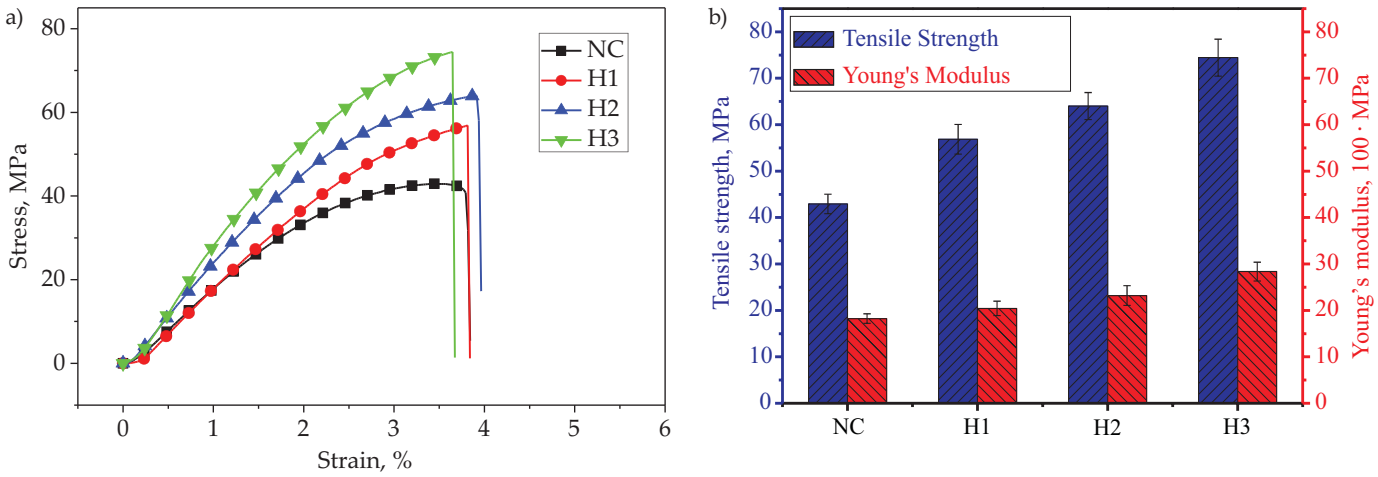

Fig. 10. Mechanical properties of prepared samples: a) stress-strain curves, b) tensile strengths and Young's moduli results

T a b l e 8. Mechanical properties of NC control sample and amino-POSS-NC hybrid materials

Sample symbol	Young's modulus, MPa	Tensile strength, MPa
NC	1823 ± 102	42.9 ± 2.1
H1	2043 ± 153	56.8 ± 3.2
H2	2319 ± 211	64.0 ± 2.9
H3	2836 ± 203	74.4 ± 4.0

ties of the material. The EDS Si mapping revealed that the amino-POSS was well dispersed throughout the NC matrix. The thermal stability of amino-POSS-NC hybrid materials was improved according to the increase of E_a value determined using the Ozawa model (from 124.98 to 165.06 kJ/mol) and Kissinger model (from 139.65 to 185.29 kJ/mol) at the maximum of amino-POSS content. TGA results also proved the improvement of thermal stability due to the delayed decomposition temperature based on the $T_{5\,\%}$ and $T_{50\,\%}$ values. The uniaxial tensile tests revealed that the introduction of amino-POSS prominently enhanced the tensile strengths and the Young's moduli, which can be respectively increased by 73.4 and 55.6 %. It was found that the introduction of thermally stable compounds with Si-O-Si frameworks and rigid silica cages as well as the good dispersion of amino-POSS contribute to the improvement of the thermal stability and mechanical properties of NC.

ACKNOWLEDGMENTS

The authors thank the National Natural Science Foundation of China (No. 21474008).

REFERENCES

[1] Jin M., Luo N., Li G., Luo Y.: *Journal of Thermal Analysis and Calorimetry* **2015**, *121* (2), 901. http://dx.doi.org/10.1007/s10973-015-4574-4

[2] Chajistamatiou A.S., Bakeas E.B.: *Talanta* **2016**, *151*, 192. http://dx.doi.org/10.1016/j.talanta.2016.01.038

[3] Mao C., Chen C.: *Journal of Applied Polymer Science* **2003**, *90* (*14*), 4000. http://dx.doi.org/10.1002/app.13121

[4] Alinat E., Delaunay N., Costanza C. *et al.*: *Talanta* **2014**, *125* (*125*), 174. http://dx.doi.org/10.1016/j.talanta.2014.02.071

[5] Ma S., Song G., Feng N.: *Carbohydrate Polymers* **2012**, *89* (*1*), 36. http://dx.doi.org/10.1016/j.carbpol.2012.02.029

[6] Bao T.N., Gautrot J.E., Nguyen M.T., Zhu X.X.: *Journal of Materials Chemistry* **2007**, *17*, 1725. http://dx.doi.org/10.1039/B616446C

[7] Gao X.F., Xu L.P., Xue Z.X. *et al.*: *Advanced Materials* **2014**, *26* (*11*), 1771. http://dx.doi.org/10.1002/adma.201304487

[8] Tanyolaç D., Özdural A.R.: *Reactive and Functional Polymers* **2000**, *45* (*3*), 235. http://dx.doi.org/10.1016/S1381-5148(00)00037-7

[9] Peterson G.R., Cychosz K.A., Matthias T., Hope-Weeks L.J.: *Chemical Communication* **2012**, *48* (*96*), 11 754. http://dx.doi.org/10.1039/c2cc36071c

[10] Zhang X., Weeks B.L.: *Journal of Hazardous Materials* **2014**, *268* (*3*), 224. http://dx.doi.org/10.1016/j.jhazmat.2014.01.019

[11] Mu X., Yu H., Zhang C. *et al.*: *Carbohydrate Polymers* **2016**, *136*, 618. http://dx.doi.org/10.1016/j.carbpol.2015.08.070

[12] Shen W., Wang H., Liu Y. *et al.*: *Colloids and Surfaces A: Physicochemical and Engineering Aspects* **2007**, *308* (*1–3*), 20. http://dx.doi.org/10.1016/j.colsurfa.2007.05.023

[13] Katoh K., Yoshino S., Kubota S. *et al.*: *Propellants, Explosives, Pyrotechnics* **2007**, *32* (*5*), 406. http://dx.doi.org/10.1002/prep.200700044

[14] Yoon J., Lee J., Choi B. *et al.*: *Nano Research* **2016**, 1. http://dx.doi.org/10.1007/s12274-016-1268-6

[15] Wolszakiewicz T., Książczak A.: *Journal of Thermal Analysis and Calorimetry* **2004**, *77*, 353. http://dx.doi.org/10.1023/B:JTAN.0000033219.39717.68
[16] Katoh K., Yoshino S., Kubota S. *et al.*: *Propellants, Explosives, Pyrotechnics* **2007**, *32* (*4*), 314. http://dx.doi.org/10.1002/prep.200700034
[17] Hassan M.A.: *Journal of Hazardous Materials* **2001**, *88* (*1*), 33. http://dx.doi.org/10.1016/S0304-3894(01)00297-7
[18] Moniruzzaman M., Bellerby J.M.: *Polymer Degradation and Stability* **2008**, *93* (*6*), 1067. http://dx.doi.org/10.1016/j.polymdegradstab.2008.03.020
[19] Katoh K., Higashi E., Nakano K. *et al.*: *Propellants, Explosives, Pyrotechnics* **2010**, *35* (*5*), 461. http://dx.doi.org/10.1002/prep.200900074
[20] Qian X., Song L., Jiang S. *et al.*: *Industrial & Engineering Chemistry Research* **2013**, *52* (*22*), 7307. http://dx.doi.org/10.1021/ie400872q
[21] Chen Y., Peng Y., Liu W.Y. *et al.*: *Advanced Materials Research* **2013**, *741*, 28. http://dx.doi.org/10.4028/www.scientific.net/AMR.741.28
[22] Wu G., Chen L., Liu L.: *Journal of Materials Science* **2016**, *52* (*2*), 1. http://dx.doi.org/10.1007/s10853-016-0401-y
[23] Blattmann H., Mülhaupt R.: *Macromolecules* **2016**, *49* (*3*), 742. http://dx.doi.org/10.1021/acs.macromol.5b02560
[24] Montero B., Bellas R., Ramírez C. *et al.*: *Composites Part B: Engineering* **2014**, *63*, 67. http://dx.doi.org/10.1016/j.compositesb.2014.03.023
[25] Mirmohammadi S.A., Nekoomanesh-Haghighi M., Gezaz S.M. *et al.*: *Materials Science and Engineering: C* **2016**, *68*, 530. http://dx.doi.org/10.1016/j.msec.2016.06.027
[26] Gidden J., Kemper P.R., Shammel E. *et al.*: *International Journal of Mass Spectrometry* **2003**, *222* (*1–3*), 63. http://dx.doi.org/10.1016/S1387-3806(02)00951-X
[27] Zong P., Fu J., Chen L. *et al.*: *RSC Advances* **2016**, *6* (*13*), 10 498. http://dx.doi.org/10.1039/c5ra24885j
[28] Vahabi H., Ferry L., Longuet C. *et al.*: *Materials Chemistry and Physics* **2012**, *136* (*2–3*), 762. http://dx.doi.org/10.1016/j.matchemphys.2012.07.053
[29] Girouard N.M., Xu S., Schueneman G. *et al.*: *ACS Applied Materials & Interfaces* **2016**, *8* (*2*), 1458. http://dx.doi.org/10.1021/acsami.5b10723
[30] Trache D., Khimeche K., Mezroua A., Benziane M.: *Journal of Thermal Analysis and Calorimetry* **2016**, *124* (*3*), 1485. http://dx.doi.org/10.1007/s10973-016-5293-1
[31] Chen S., Gao J., Han H., Wang C.: *Iranian Polymer Journal* **2014**, *23* (*8*), 609. http://dx.doi.org/10.1007/s13726-014-0255-6
[32] Dong H., Brennan T.D.: *Chemistry of Materials* **2006**, *18* (*17*), 4176. http://dx.doi.org/10.1021/cm060509e
[33] Nikolić A., Petrović S., Antonović D., Gobor L.: *Journal of Molecular Structure* **1997**, *408–409*, 355.
[34] Lee Y.J., Kuo S.W., Su Y.C. *et al.*: *Polymer* **2004**, *45* (*18*), 6321. http://dx.doi.org/10.1016/j.polymer.2004.04.055
[35] Li R., Xu H., Hu H. *et al.*: *Journal of Energetic Materials* **2014**, *32* (*1*), 50. http://dx.doi.org/10.1080/07370652.2012.754515
[36] Fan H., Yang R.: *Industrial & Engineering Chemistry Research* **2013**, *52* (*7*), 2493. http://dx.doi.org/10.1021/ie303281x
[37] Chen S., Guo L., Du D., Li X.: *Polymer* **2016**, *103*, 27. http://dx.doi.org/10.1016/j.polymer.2016.09.034
[38] Bu X., Zhou Y., Huang F.: *Materials Letters* **2016**, *174* (*1*), 21. http://dx.doi.org/10.1016/j.matlet.2016.03.067
[39] Wang K., Liu D., Xu S., Cai G.: *Thermochimica Acta* **2015**, *610*, 23. http://dx.doi.org/10.1016/j.tca.2015.04.022
[40] Ozawa T.: *Journal of Thermal Analysis* **1970**, *2* (*3*), 301. http://dx.doi.org/10.1007/BF01911411
[41] Pourmortazavi S.M., Hosseini S.G., Nasrabadi M.R. *et al.*: *Journal of Hazardous Materials* **2009**, *162* (*2–3*), 1141. http://dx.doi.org/10.1016/j.jhazmat.2008.05.161
[42] Kissinger H.E.: *Analytical Chemistry* **1957**, *29* (*11*), 1702. http://dx.doi.org/10.1021/ac60131a045
[43] Teo J.K.H., Teo K.C., Pan B. *et al.*: *Polymer* **2007**, *48* (*19*), 5671. http://dx.doi.org/10.1016/j.polymer.2007.07.059
[44] Sovizi M.R., Hajimirsadeghi S.S., Naderizadeh B.: *Journal of Hazardous Materials* **2009**, *168* (*2–3*), 1134. http://dx.doi.org/10.1016/j.jhazmat.2009.02.146
[45] Jeon J.H., Tanaka K., Chujo Y.: *Journal of Materials Chemistry A* **2014**, *2* (*3*), 624. http://dx.doi.org/10.1039/C3TA14039C
[46] Zhao C., Yang X., Wu X. *et al.*: *Polymer Bulletin* **2008**, *60* (*4*), 495. http://dx.doi.org/10.1007/s00289-008-0887-9
[47] Yang X., Li Y., Wang Y. *et al.*: *Journal of Polymer Research* **2017**, *24*, 50. http://dx.doi.org/10.1007/s10965-017-1203-x
[48] Yuan D.D., Cai X.F.: *Chinese Journal of Polymer Science* **2013**, *31* (*10*), 1352. http://dx.doi.org/10.1007/s10118-013-1306-8
[49] Wang X., Romero M.Q., Zhang, X.Q. *et al.*: *RSC Advances* **2015**, *5*, 10 647. http://dx.doi.org/10.1039/C4RA14943B
[50] Puziy A.M., Poddubnaya O.I., Ziatdinov A.M.: *Applied Surface Science* **2006**, *252* (*23*), 8036. http://dx.doi.org/10.1016/j.apsusc.2005.10.044
[51] Huang G., Liang H., Wang Y. *et al.*: *Materials Chemistry and Physics* **2012**, *132* (*2–3*), 520. http://dx.doi.org/10.1016/j.matchemphys.2011.11.064
[52] Puziy A.M., Poddubnaya O.I., Socha R.P. *et al.*: *Carbon* **2008**, *46* (*15*), 2113. http://dx.doi.org/10.1016/j.carbon.2008.09.010

[53] Tsai K.C., Kuan C.F., Chen C.H. *et al.*: *Journal of Applied Polymer Science* **2013**, *127* (*2*), 1084. http://dx.doi.org/10.1002/app.37700
[54] Hu L., Jiang P., Bian G. *et al.*: *Journal of Applied Polymer Science* **2016**. http://dx.doi.org/10.1002/APP.44440
[55] Yin G., Chen G., Zhou Z., Li Q.: *RSC Advances* **2105**, *5* (*42*), 33 356. http://dx.doi.org/10.1039/c5ra01971k
[56] Tanaka K., Adachi S., Chujo Y.: *Journal of Polymer Science Part A: Polymer Chemistry* **2009**, *47* (*21*), 5690. http://dx.doi.org/10.1002/pola.23612

Received 16 XII 2016.